Writhing Geometry at Finite Temperature: Random Walks and Geometric phases for Stiff Polymers

A.C. Maggs.
PCT, ESPCI, 10 Rue Vauquelin, Paris, 75005.

November 10, 2000

Abstract

I study the geometry of a semiflexible polymer at finite temperatures. The writhe can be calculated from the properties of Gaussian random walks on the sphere. We calculate static and dynamic writhe correlation functions. The writhe of a polymer is analogous to geometric or Berry phases studied in optics and wave mechanics. Our results can be applied to confocal microscopy studies of stiff filaments and to simulations of short DNA loops.

1 Introduction

Experiments which micro-manipulate stiff polymers, such as actin filaments or DNA have lead to a renewed interest in the static and dynamic properties of semiflexible polymers. This article treats the writhing properties of stiff polymers, in particular those which have a length comparable to the persistence length. The static and dynamic writhing properties discussed here can be easily measured using confocal microscopy on fluorescently marked actin filaments for which the persistence length is $15\mu\mathrm{m}$, and which are readily available in a range of length varying between $5\mu\mathrm{m}$ to $30\mu\mathrm{m}$.

In this article I concentrate almost exclusively on the writhing fluctuations of polymers; clearly a stiff polymer has both bending and twisting degrees of freedom, but it is known [1, 2, 3] that the relaxation times of the twist modes are much faster than those of bending modes, which drive the writhe dynamics. Thus the longtime effective degrees of freedom of a fluctuating stiff polymer are those of writhe discussed here.

At finite temperatures the trajectory of a semiflexible filament is not smooth and direct application of the standard relationships between, for instance geometric torsion and writhe turns out to be quite subtle. Indeed the usual definition of torsion requires curves that are $\mathcal{C}^3$, whereas the trajectory of a thermalized stiff polymer is much less smooth than this; in fact both the torsion and its integral are divergent so that the usual relationship between writhe $\mathcal{W}\mathrm{r}$ and torsion τ, $2\pi\mathcal{W}\mathrm{r} + \oint \tau \mathrm{ds} \ = 0 \bmod 2\pi$, is useless. Here we explore representations of the trajectory of a polymer based on random walks on the sphere. We are able to use this representation to calculate the static and dynamic fluctuations of a stiff polymer. We discuss the analogy between Fuller's result for the writhe of a polymer and the geometric phase known from quantum and optical physics.

The main quantitative predictions made in this paper are for the static and dynamic correlation functions for the writhe, $\mathcal{W}\mathrm{r}$ in several different geometries. In particular we calculate $\langle \mathcal{W}\mathrm{r}^2 \rangle$ and $\langle (\mathcal{W}\mathrm{r}(\mathrm{t}) - \mathcal{W}\mathrm{r}(0))^2 \rangle$ for open and closed semiflexible polymers. With these results we are able to understand quantitatively a number of results for writhe autocorrelation functions which have been measured recently in numerical models of DNA [4]. We also show that short, highly curved sections of polymer give enhanced contributions to the writhe of a polymer. We explicitly calculate the probability distribution for writhing, $\mathcal{P}_{\mathcal{K}}(\mathcal{W}\mathrm{r})$ for short polymers and show that it is strongly non-Gaussian.

2 Writhe of a curve

Consider fig. (1). It represents a solid bar that has been bent three times by 90°. On one face of the bar I have added an unit arrow, $\mathbf{n}$, which is perpendicular to the local tangent of the bar, $\mathbf{t}$. Following the

motion of $\mathbf{n}$ as we move along the bar we notice that after the triple bend there has been a rotation of the arrow by 90° about the vertical axis despite the fact that $\mathbf{t}$ has come back to its original direction. This rotation is due to the *writhe* of the path. Mathematicians measure writhe in units of 2π. Thus fig. (1) corresponds to a writhe, $\mathcal{W}\mathsf{r}$ of $1/4$.

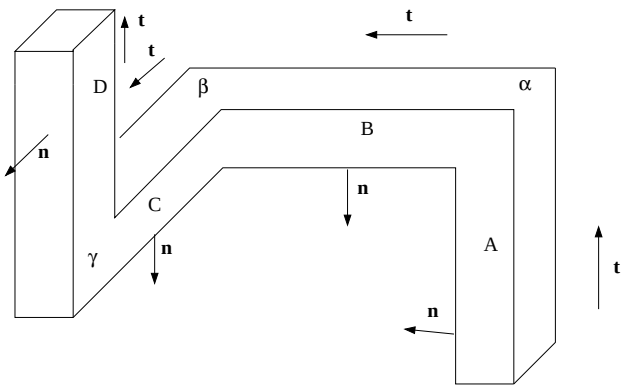

Figure 1: A bar is bent three times, leading to a rotation of 90° of the vector $\mathbf{n}$ marking one face of the prism. This rotation is due to the writhing of the shape in three dimensions.

The writhing in fig. (1) can be best understood by studying the geometry of the tangent vector $\mathbf{t}$ together with the normal vector $\mathbf{n}$. Since the vector $\mathbf{t}$ has unit magnitude, is thus lives on a unit sphere, $\mathcal{S}_2$, drawn in figure (2). The vector $\mathbf{n}$ is perpendicular to $\mathbf{t}$: it must always remain tangential to the sphere. The geometry of the bent bar in fig. (1) has been translated onto $\mathcal{S}_2$ in fig. (2): Start at bottom right of fig. (1) and move vertically, following the vector $\mathbf{t}$. The whole vertical section, A corresponds to a single point on the sphere, the north pole. Passing through the first bend α corresponds to the arc, also labeled α on the sphere. The second straight section of the bar, B points to the left and corresponds to the point B on the left most edge of the sphere. Despite the *discontinuities* in the direction of bar the vector $\mathbf{n}$ is always *continuous* on $\mathcal{S}_2$. The vector $\mathbf{n}$ is *parallel transported* around a loop on the sphere.

The rotation of the vector $\mathbf{n}$ is a manifestation of the *curvature* of the sphere. Parallel transport of a vector around a closed path on a surface leads to a angle between the initial and final vectors. For a two dimensional surface this angle is given by

$$\Delta_\Omega = \int \mathsf{K}\ \mathsf{dS} \quad \text{modulo } 2\pi\ , \tag{1}$$

where K is the Gaussian curvature of the surface and the integral is over the region enclosed by the path. For a sphere the Gaussian curvature is equal to unity so that the angle of rotation between two ends of a bent prism is calculated from the area enclosed by the trajectory on the sphere. This is just the contents of Fuller's result [5]. In our simple example the solid angle enclosed by the the curve (α, β, γ) is $\pi/2$ leading to the rotation of $\mathbf{n}$ by 90°.

Any real prism, made of an elastic material has an additional degree of freedom associated with it: At any point it can be twisted, at angular velocity $\omega_{\mathbf{t}}(\mathsf{s})$ about the tangent, compared with the parallel transported frame shown in figures (1,2). Clearly the total rotation in the laboratory frame is given as the sum of the rotation due to the writhing, plus the rotation $\int \omega_{\mathbf{t}}\ \mathsf{ds}$ coming from the relative motion of the parallel transported and twisting frame. This is the content of White's theorem [6] for a curve. $\mathcal{L}\mathsf{n} = \mathcal{W}\mathsf{r} + \mathcal{T}w$, where $2\pi\mathcal{L}\mathsf{n}$ is the total rotation, $2\pi\mathcal{T}w$ the rotation due to twisting and $2\pi\mathcal{W}\mathsf{r}$ the rotation due to writhing.

3 Geometry of three dimensional curves

In this section I shall review some of the elementary properties of a line in three dimensions, pointing out the relationships between different representations of the geometry. In particular I will discuss the classic choice of the Frenet frame and compare it with the parallel transported frame of fig. (1,2) to show how the two descriptions are related.

At each point of the curve associate three orthogonal unit vectors $\{\mathbf{t}, \mathbf{n}, \mathbf{b}\}$. The vector $\mathbf{t}$ is tangent to the curve, while $\mathbf{n}$ and $\mathbf{b}$ are perpendicular to the tangent, they both live in the surface of the sphere of fig. (2). A theorem of Euler [7] then shows that the motion of this frame as a function of s, the curvilinear distance, is a pure rotation. Thus grouping the vectors into a matrix, $\mathbf{M}$ gives

$$\frac{\mathrm{d}\mathbf{M}}{\mathrm{ds}} = \Omega.\mathbf{M} \tag{2}$$

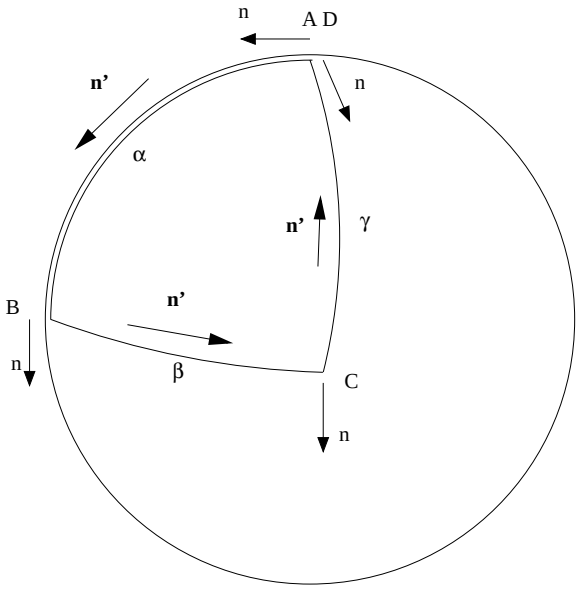

Figure 2: Trajectory in the tangent space. The points A, B, C, D correspond to the straight sections of the prism in fig. (1). The three bends correspond to the geodesic arcs α, β, γ. The vector $\mathbf{n}$ is parallel transported along the path, leading to an angle of $\pi/2$ between the initial and final vectors $\mathbf{n}$. The vector $\mathbf{n}'$ (corresponding to the Frenet frame) always points in the direction of motion on the sphere.

with Ω anti-symmetric. Different choices are possible; we shall now discuss two: firstly the classic Frenet frame, known from elementary treatments of line geometry in three dimensions, secondly the choice of parallel transport corresponding to fig. (1).

The most common choice for the rotation matrix, is the following corresponding to the Frenet frame [8],

$$\Omega = \begin{pmatrix} 0 & \kappa & 0 \\ -\kappa & 0 & \tau \\ 0 & -\tau & 0 \end{pmatrix} . \tag{3}$$

This representation is particularly useful because $1/\kappa$ has a simple geometric interpretation: it is the radius of curvature of the line at the point s. The element τ is known as the *torsion*.

As shown above the geometry of three dimensional curves becomes easier to understand if we work in the tangential space $\mathcal{S}_2$. What is the geometric picture that corresponds to the choice of the matrix in eq. (3)? On the sphere, the curve $\mathbf{t}(s)$ moves at speed κ in the direction $\mathbf{n}'$ which is parallel to $d\mathbf{t}/ds$. As a function of s the vector $\mathbf{n}'$ rotates in the surface at angular velocity $\omega_{\mathbf{t}} = \tau$. Since we are particularly interested in the internal geometry of the sphere let us now transform the parameterization of the curve from unit speed in real space to to a unit speed curve on the sphere. The element of length transforms as $d\sigma = \kappa ds$; the angular velocity of $\mathbf{n}'$ expressed as a function of σ (rather than s) is τ/κ. In fig. (2) τ/κ is zero along the arcs α, β, γ but at the corners, A, B and C there is a rapid rotation of $\mathbf{n}'$ by $90°$, corresponding to a delta-function singularity in the angular velocity. The representation becomes *singular* in for curves which are not sufficiently smooth, or for curves where κ passes through zero.

The second representation of the geometry (sometimes known as the Fermi-Walker frame), [9] is the following

$$\Omega = \begin{pmatrix} 0 & \alpha & \beta \\ -\alpha & 0 & 0 \\ -\beta & 0 & 0 \end{pmatrix} . \tag{4}$$

It corresponds to the geometry shown in figures (1, 2). In this frame the vectors $\mathbf{n}$ and $\mathbf{b}$ are parallel transported: The original definition [10] of parallel transport of a vector $\mathbf{v}$ (due to Levi-Civita) is that the rate of change of the vector, projected back on to the tangent plane is zero. For our space curve this corresponds to the equation

$$\frac{d\mathbf{v}}{d\sigma} - \mathbf{t}\left(\mathbf{t}.\frac{d\mathbf{v}}{d\sigma}\right) = 0. \tag{5}$$

We see that both $\mathbf{n}$ and $\mathbf{b}$ (as well as an arbitrary, constant linear combination of $\mathbf{b}$ and $\mathbf{n}$) evolving with the matrix eq. (4) obey this equation. In figure (2) the vector $\mathbf{n}$ is translated in such a way that $d\mathbf{n}/d\sigma$ is always normal to the surface, in agreement with this definition.

For sufficiently regular curves both representations are equivalent. At each point on the curve perform a rotation about the vector $\mathbf{t}$ in the following manner:

$$\begin{pmatrix} \mathbf{n}' \\ \mathbf{b}' \end{pmatrix} = \begin{pmatrix} \cos\theta & \sin\theta \\ -\sin\theta & \cos\theta \end{pmatrix} \begin{pmatrix} \mathbf{n} \\ \mathbf{b} \end{pmatrix} , \tag{6}$$

where $\mathbf{n}'$ and $\mathbf{b}'$ are the vectors in the description eq. (3) and $\mathbf{n}$ and $\mathbf{b}$ are the vector in the description of eq. (4). The two representations are be linked by setting

$$\dot{\theta} = \tau \tag{7}$$

$$\alpha = \kappa\cos\theta \tag{8}$$

$$\beta = \kappa\sin\theta . \tag{9}$$

Consider an arbitrary trajectory on the sphere comparing the two frames, starting from a common initial vector $\mathbf{n}(0)$. After the loop there has been a rotation of

$$\theta_L = \oint \frac{\tau}{\kappa}\, d\sigma = \oint \tau\, ds \tag{10}$$

between the two description. Note that the integral is about the whole closed trajectory on the sphere, including the extra boundary turn needed to spin $\mathbf{n}'(0)$ to $\mathbf{n}'(L)$. We shall use the sign "$\oint$" to designate such integral from now on this this article. In real space this corresponds to adding a boundary correction equal the the difference in angle between the principle curvatures at the two ends of the polymer. If the angle between the parallel transported frames $\mathbf{n}(0)$ and $\mathbf{n}(L)$ is Δ_Ω then the angle between $\mathbf{n}(0)$ and $\mathbf{n}'(L)$ is $(\Delta_\Omega + \theta_L)$. Clearly this must be equal to a multiple of 2π. Thus we deduce

$$\Delta_\Omega + \oint \frac{\tau}{\kappa}\, d\sigma = 2n\pi\ , \tag{11}$$

which when combined with equation (1) is the Gauss-Bonnet theorem for a sphere.

3.1 Local Geometry

Locally a smooth writhing curve can be written in the following form

$$\mathbf{r}(u) = \left(-\frac{\kappa\tau}{6}s^3, \frac{\kappa}{2}s^2, s\right)\ , \tag{12}$$

showing that $\kappa\tau$ measures the rate at which the curve becomes non-planar. We have chosen local coordinates so that the tangent points in the $\hat{\mathbf{e}}_z$ direction. From this expression we see that a straight filament with $\kappa = 0$ can be approached with an arbitrary value of the torsion τ.

On $\mathcal{S}_2$ we find that $\mathbf{t} \approx (-\kappa\tau s^2/2, \kappa s, 1)$. When we transform to unit speed on $\mathcal{S}_2$ using $\kappa s = \sigma$ we find

$$\mathbf{t} \approx \left(-\frac{\tau}{2\kappa}\sigma^2, \sigma, 1\right)\ , \tag{13}$$

so that the projection of the path from the sphere onto the tangent plane is curved, with radius of curvature κ/τ. Thus τ/κ has a natural interpretation on the sphere and is indeed the *geodesic curvature* of the trajectory on $\mathcal{S}_2$.

4 Examples of Writhe

4.1 Bent Bar

The trajectory on the sphere, shown in in fig. (2) has three rotations of $\pi/2$ corresponding to each bend in the bar thus $\oint(\tau/\kappa)\ d\sigma = 3\pi/2$. Δ_Ω is also equal to $\pi/2$ as is the area enclosed by the curve on the sphere as required by eq (1). Thus $2\pi\mathcal{W}r + \oint \tau\ ds = 2\pi$.

4.2 Circular Helix

A second example is a long helix, parameterized by the equation

$$\mathbf{r}(u) = (a\cos u, a\sin u, u) \tag{14}$$

for the case a small. The torsion is given by

$$\tau = \frac{1}{1+a^2} \tag{15}$$

with $ds = du\sqrt{1+a^2}$. As a function of s the trajectory of $\mathbf{t}$ on the sphere is a circle or radius a. Consider the various contributions to eq. (11) for a line of length $L = 2\pi N\sqrt{1+a^2}$, so that the are N complete helical repeats. The integral of the torsion is given by

$$\int_0^L \frac{ds}{1+a^2} \approx 2N\pi - N\pi a^2 + O(a^4)\ . \tag{16}$$

The result is at first very surprising. In the limit $a \to 0$ the helix becomes a straight line, however the torsion and its integral remains finite: The straight reference state is singular for the calculation of the torsion of a curve.

This second example shows that the torsion is sensitive to small scale details in the representation of a curve, in particular to small scale helical structure (as is found in stiff biomolecules). At finite temperature the situation is even more delicate. Even for a filament with a linear ground state small scale structure is excited by thermal fluctuations so that the integral of the torsion is badly behaved. In fact the standard relationships between writhe and torsion, lead to large, uninteresting zero order contributions which mask the interesting higher order term, as found here for a simple helix.

The enclosed area by the path $\mathbf{t}(s)$, is better behaved than the torsion so that we can use eq. (1) and the fact that the circle of area πa^2 is traversed N times to find $\Delta_\Omega = N\pi a^2$. The total rotation, which

is physically interesting, corresponds to the second order term in a^2 appearing in eq. (16). We conclude that it is better to calculate the writhe from Fuller's result on the enclosed area of the curve $\mathbf{t}(s)$, rather than from the integrated torsion. We now generalize these remarks to finite temperature.

5 Alternative Formulations of Writhe

In much numerical work on the writhe of polymers one uses the following double integral representation of the writhe:

$$\mathcal{W}r = \frac{1}{4\pi}\int ds \int ds' \frac{\mathbf{r}(s)-\mathbf{r}(s')}{|\mathbf{r}(s)-\mathbf{r}(s')|^3}.\frac{d\mathbf{r}(s)}{ds}\times\frac{d\mathbf{r}(s')}{ds'}. \tag{17}$$

A very elegant link to the above description of the writhe as parallel transport along the trajectory $\mathbf{t}(s)$ has been given by Hannay [11]. The integral (17) calculates the area swept out on a sphere by the vector

$$\hat{\mathbf{e}}(s,s') = \frac{\mathbf{r}(s)-\mathbf{r}(s')}{|\mathbf{r}(s)-\mathbf{r}(s')|} \tag{18}$$

as a function of the two variables s and s' which are now to be considered as a generalized, non-orthogonal coordinate system on $\mathcal{S}_2$. We now note that as $s'\to s+$ then $\hat{\mathbf{e}}\to\mathbf{t}(s)$. Similarly as $s'\to s-$ we discover that $\hat{\mathbf{e}}\to-\mathbf{t}(s)$. Thus for fixed s the curve $\hat{\mathbf{e}}(s,s')$ is a line on $\mathcal{S}_2$ from $\mathbf{t}(s)$ to $-\mathbf{t}(s)$. We can use the local description eq. (15) to show that for $(s-s')$ small

$$\hat{\mathbf{e}}(s,s') = \left(-\kappa\tau\frac{(s^2+s'^2+ss')}{6}, \kappa\frac{(s+s')}{2}, 1\right) \tag{19}$$

where we have chosed a coordinate system locally such that the tangent is along the z-axis. Transforming to intrinsic coordinates on the sphere and writing $\eta=(\sigma+\sigma')/2$ and $\eta'=(\sigma-\sigma')/2$ we see that

$$\hat{\mathbf{e}}(s,s') = \left(\frac{-\tau}{\kappa}\left(\frac{\eta^2}{2}+\frac{\eta'^2}{6}\right),\eta,1\right) \tag{20}$$

$$= \mathbf{t}(\eta) - (0,\tau\eta'^2/6\kappa,0) \tag{21}$$

The tangent is thus a local extremum for the ensemble $\hat{\mathbf{e}}(s,s')$ and for sufficiently regular curves the integral measures the area *between* the curves $\mathbf{t}(s)$ and -$\mathbf{t}(s)$. Thus we discover a direct geometric relationship to the above treatement by parallel transport where the writhe is found from the area *inside* $\mathbf{t}(s)$ and the expression eq. (17) corresponding to the area *outside* of $\mathbf{t}(s)$.

6 Bending of stiff polymers

6.1 Energetics

The bending energy of a stiff polymer is written in the form

$$E = \frac{\mathcal{K}}{2}\int\left(\frac{d\mathbf{t}(s)}{ds}\right)^2 ds\ , \tag{22}$$

where $\mathcal{K}$ is the bending modulus of the polymer. Let the energy be measured in units of the temperature then $\mathcal{K}$ is the persistence length of the polymer. This energy is completely analogous to that used in the theory of *flexible* polymers [12]

$$E_{flex} = \frac{\Sigma}{2}\int\left(\frac{d\mathbf{r}(s)}{ds}\right)^2 ds\ , \tag{23}$$

except that it is written in terms of the tangent vector $\mathbf{t}$ rather than the real space position $\mathbf{r}$. The energy (23) describes a Gaussian polymer with end to end distance $\langle R^2\rangle = 3L/\Sigma$. Like a flexible polymer the distribution of density $P(\mathbf{t},s)$ obeys a diffusion like Fokker-Planck equation [12].

$$\frac{\partial P(\mathbf{t},s)}{\partial s} = \frac{1}{2\mathcal{K}}\nabla^2_\sigma P(\mathbf{t},s)\ , \tag{24}$$

where ∇^2_σ is the Laplacian operator on the sphere. As a function of s the vector $\mathbf{t}$ diffuses with diffusion coefficient $1/(2\mathcal{K})$. The typical separation on $\mathcal{S}_2$ of two points separated by a curvilinear distance s in real space is

$$R^2_\sigma = 2s/\mathcal{K}, \tag{25}$$

when $s\ll\mathcal{K}$.

From the result eq. (24) we understand why torsion, τ is poorly defined at finite temperatures: Consider a discretization of a semiflexible polymer with sections of length a in real space. On the sphere the polymer is represented as a random walk with points separated by a distance comparable to $\sqrt{a/\mathcal{K}}$. The direction of each step on the sphere is completely *uncorrelated* with its neighbors. Thus the angle between successive links is of order of one radian. There are L/a sections so that the torsion locally has a value $\tau\sim\pm 1/a$ and $\int\tau ds\sim\pm\sqrt{L/a}$ which diverges with the cutoff. The physically interesting writhe is thus

hidden by the diverging zero order fluctuations. This is similar to the example of the helix above where the physically interesting writhe was hidden by the small amplitude helical pitch. We shall now show that despite some subtleties the angle between the vectors $\mathbf{n}(0)$ and $\mathbf{n}(L)$ is calculated from the area enclosed by the random walk on $\mathcal{S}_2$.

This result is linked with the natural class of functions for which the Frenet frame is defined. Bishop [13] showed that the Frenet frame (and thus the torsion) requires a function space of $\mathcal{C}^3$ curves. The frame defined by parallel transport has lower smoothness requirements. Clearly a semiflexible polymer, which is only $C^{3/2}$, is too rough for the Frenet frame to be useful. It would be interesting to better understand the representation eq. (17) for the writhe at finite temperatures. The simple picture of Hannay seems to rely on the regularity of τ so that the curve $\mathbf{t}(s)$ is extremal for the set of vectors $\hat{\mathbf{e}}(s, s')$.

6.2 Short Polymers

Consider a polymer with the following boundary conditions: The ends of the filament $\mathbf{r}(0)$ and $\mathbf{r}(L)$ are free to move but the chain is constrained by external couple so that $\mathbf{t}(0)$ and $\mathbf{t}(L)$ point in the $\hat{\mathbf{z}}$ direction, as in fig. (1). The trajectory is closed on the sphere (but open in real space). If the polymer is short, ($L \ll \mathcal{K}$) the trajectory never moves too far from the north pole; locally the geometry of the sphere remains Euclidean. The writhe of the filament can thus be calculated from the area enclosed by a closed Gaussian loop in a plane. This problem has been treated by Levy [14]. The enclosed area, fig. (4), scales in the same manner as R_σ^2 but is randomly signed (depending on whether the path is traversed clockwise or anti-clockwise). The mean squared area has a non-zero average:

$$\langle \mathcal{W}r^2 \rangle = \frac{L^2}{48\mathcal{K}^2} \ . \tag{26}$$

In fact the whole probability distribution is known and is given by

$$\mathcal{P}_{\mathcal{K}}(\mathcal{W}r) = \frac{\pi\mathcal{K}}{L} \frac{1}{\cosh^2(2\pi\,\mathcal{W}r\,\mathcal{K}/L)} \quad . \tag{27}$$

Although the distribution of the size of the loops is Gaussian the distribution of the writhe has wings which are simple exponentials, implying that the free energy of a strongly writhing state varies linearly with $\mathcal{W}r$,

$$F = 4\pi\mathcal{K}\,\mathcal{W}r/L \, . \tag{28}$$

This result implies that there is a critical torque $\Gamma = 2\mathcal{K}/L$, which destabilizes fluctuations about the ground state of the polymer.

For an elastic filaments with torsional elastic constant T the total angle of rotation between two ends of a polymer is given by the sum of the writhing and twisting contributions. The twisting contribution, θ is Gaussian distributed:

$$\mathcal{P}_T(\theta) = \sqrt{\frac{T}{2\pi L}} e^{-\theta^2 T/2L} \ . \tag{29}$$

We find the distribution of the total rotation angle φ from a convolution of the writhe and twist distributions

$$\mathcal{P}(\varphi) = \int \mathcal{P}_{\mathcal{K}}(\mathcal{W}r)\,\mathcal{P}_T(\theta)\,\delta(2\pi\mathcal{W}r + \theta - \varphi)\ d\mathcal{W}r\ d\theta \ . \tag{30}$$

The twisting and writhing distributions are plotted in fig. (3).

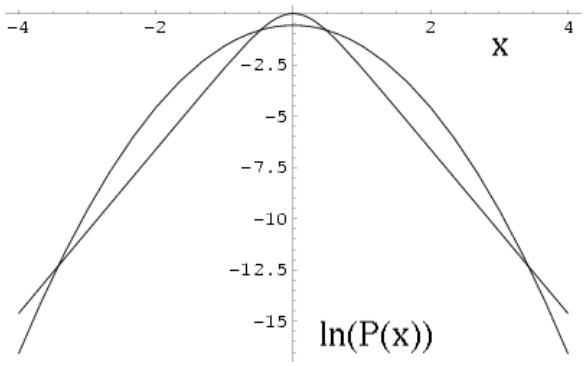

Figure 3: Distribution functions eq. (27), (29) of angle of rotation,x (on a log-linear scale) due to writhe and twist. The parabolic curve is the distribution of twist, the curve with the exponential wings is the distribution of rotation due to writhe. Plot is for $T/L = \mathcal{K}/L = 2$

6.3 Long Polymers

The writhe properties of long semiflexible polymers have been extensively studied in the context of DNA super-coiling [15, 16, 17]. It is known from numerical simulations that for long semiflexible polymers $\langle \mathcal{W}r^2 \rangle \sim L$. Recently, detailed analytic calculations

[18] have shown that this is only true in models with a microscopic cut off. In the absence of a cut off the writhe fluctuations are logarithmically divergent. How do we understand these results from our picture of a stiff polymer as a random walk on the sphere?

As shown by Fuller [5] the writhe of an arbitrary configuration of a polymer is found from the expression

$$\mathcal{W}r = \frac{1}{2\pi}\int \frac{(\mathbf{t}_0 \times \mathbf{t})}{1+\mathbf{t}.\mathbf{t}_0}.\ d\mathbf{t} \tag{31}$$

where $\mathbf{t}_0$ is an arbitrary constant vector. This expression is valid when the path $\mathbf{t}(s)$ can be deformed from the vector $\mathbf{t}_0$ without the denominator vanishing. Let $\mathbf{t}_0$ point in the direction of the north pole then the singularity is at the south pole. To understand the nature of the singularity expand about the south pole so that

$$\mathbf{t} \approx (u, v, -1 + u^2/2 + v^2/2) \tag{32}$$

with both u and v small. The contribution to the writhe coming from a section of polymer near the south pole has the following form

$$\Delta\mathcal{W}r \approx \frac{1}{\pi}\int \frac{u\,dv - v\,du}{u^2+v^2} = \frac{1}{\pi}\int d\phi\ , \tag{33}$$

where ϕ is the azimuthal angle of the path subtended at the south pole. The contribution of the polymer to the writhe near the pole is twice the winding number about the pole. This winding number is clearly discontinuous as a function of the position of a path: A small circle centered at the pole has winding number unity. If it is displaced more than its radius the winding number jumps to zero.

We conclude that small fluctuations in the direction of the polymer can give important ($O(1)$) fluctuations in the total writhe if they occur near the south pole. The distribution of winding of a random walk on a sphere has been given analytically [19, 20]. It is known that the distribution is wide and has a Cauchy tail. This is due to the fact that in a close approach to the pole to within a distance ϵ there are typically $\sqrt{\log \epsilon}$ rotations about the pole. This is the origin of the Cauchy tail in the writhe fluctuations which decays even more slowly than the curve plotted in fig. (3) [18].

Is this singularity at the south pole important for short polymers? When the polymer is very short transit in the region of the south pole is strongly suppressed since a bend of 180° costs an energy $\pi^2\mathcal{K}/2L$ leading to exponentially small corrections to the law (26). However as soon as $L \sim \mathcal{K}$ the dense nature of random walk in two dimensions means that with high probability there is a point on the polymer which is very close to the south pole, giving a strong Cauchy tail to the writhe distribution.

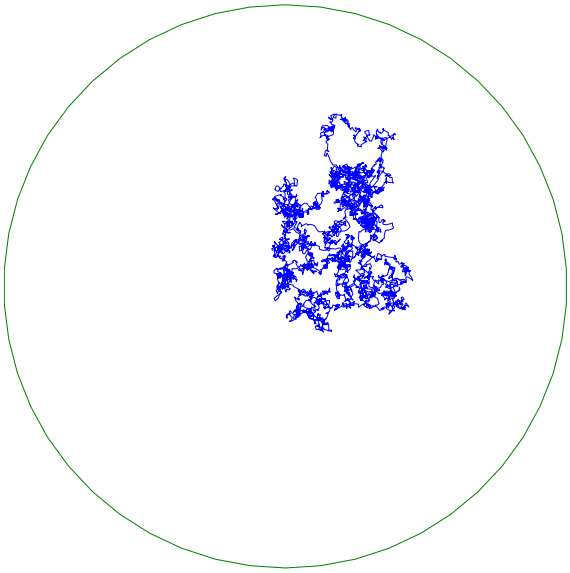

Figure 4: Realization of a closed random walk on a sphere. The walk has a fractal nature with detail on all length scales. The area enclosed by the loop will be dominated by the largest loops in the above figure so that the area enclosed scales as the radius of gyration squared.

7 Writhing dynamics

When studying the dynamics of writhing of stiff polymer the representation of the writhe given by eq. (31) is only useful for filaments which are much shorter than the persistence length. Motion of a long polymer is almost surely going to cause passage of the path over the south pole leading to a discontinuous contribution to the writhe. It is better to use the generalization [5] of eq. (31)

$$\mathcal{W}r(\mathbf{t}_2) - \mathcal{W}r(\mathbf{t}_1) = \frac{1}{2\pi}\int \frac{\mathbf{t}_1 \times \mathbf{t}_2}{1+\mathbf{t}_1.\mathbf{t}_2}\ .(\dot{\mathbf{t}}_1 + \dot{\mathbf{t}}_2)\ ds\ . \tag{34}$$

Let the trajectory $\mathbf{t}_1(s)$ to be the polymer at $t = 0$ and $\mathbf{t}_2(s)$ is the trajectory at some later time. This expression remains valid until a time such that a point

on $\mathbf{t}(s)$ rotates 180° leading to a singularity in the integral.

The motion of a semiflexible filament is given by the Langevin equation [21]

$$4\pi\eta\frac{\partial \mathbf{r}_\perp}{\partial t} = -\mathcal{K}\frac{\partial^4 \mathbf{r}_\perp}{\partial s^4} + \mathbf{f}_\perp(t,s)\ . \qquad (35)$$

This equation has a characteristic dispersion relation $\omega \sim q^4$ so that after a time t, wavelengths out to $\ell_1 = (\mathcal{K}t/\eta)^{1/4}$ are equilibrated. Perturbations separated by more than the distance ℓ_1 have not had time to interact so that there are $N_1 = L/\ell_1$ dynamically independent sections remaining on the polymer.

What does this mean for the structure of the path $\mathbf{t}(s)$ on $\mathcal{S}_2$? From eq. (25) the length ℓ_1 in real space translates to a distance $R_1 \sim \sqrt{\ell_1/\mathcal{K}}$ on $\mathcal{S}_2$. Structure on the scale of R_1 has had time to move. We can thus imagine the structure at time t as being a series of N_1 beads of size $\sqrt{\ell_1/\mathcal{K}}$ strung out along the original path of the polymer on $\mathcal{S}_2$. The typical fluctuation in area from each bead is given by $(\Delta A) = \pm R_1^2$. To find the total fluctuation in area in time t add these N_1 independent fluctuations to find

$$\langle(\mathcal{W}r(t) - \mathcal{W}r(0))^2\rangle \sim N_1(\Delta A)^2 \sim L\ell_1/\mathcal{K}^2 \qquad (36)$$
$$\sim Lt^{1/4}\ . \qquad (37)$$

This result has been found recently in detailed numerical simulations [22]. The derivation in terms of random walks shows that the result is valid for polymers much longer than the persistence length: Indeed the result is valid for all times such that $\ell_1(t) \ll \mathcal{K}$. Beyond this time there are two sources of breakdown in the theory: Firstly the dynamics are no-longer described by a simple bending theory and secondly we also expect that rotations by 180° become important leading to a breakdown of our expression for the writhe.

Since the writhe fluctuations are the sum of a large number of independent contributions dynamic writhe fluctuations are distributed according to a Gaussian law. However there is always a exponentially small probability that the singularity in the integral occurs very rapidly so that the expressions found here is only be asymptotic, as was the case for the *static* distribution of writhe for short filaments eq. (27) found above.

8 Writhing of bent polymers

The discussion until now has been restricted to polymers which are straight in their ground states. It is known, however, that certain special sequences of DNA lead to ground states which are strongly curved. This leads to enhanced writhing [23]. Consider a polymer which bends an angle Ψ over a distance L_b in its ground states. On the sphere the ground state is a geodesic of length Ψ. We have seen above that a straight polymer is described by a diffusion like Fokker-Planck equation on the sphere. Addition of drift due to the spontaneous curvature leads to the equation

$$\frac{\partial P(\mathbf{t})}{\partial s} = \frac{\Psi}{L_b}\mathbf{v}.\nabla P + \frac{1}{2\mathcal{K}}\nabla_\sigma^2 P(\mathbf{t})\ , \qquad (38)$$

with $\mathbf{v}$ a unit vector describing the direction of the bend. We take as our reference configuration $\mathbf{t}_1$ the ground state and the state $\mathbf{t}_2$ the thermalized polymer. As shown above the typical fluctuations of the filament on $\mathcal{S}_2$ scale as $R_b \sim \sqrt{L_b/\mathcal{K}}$ so that the area enclosed by the pair of paths $\mathbf{t}_1$ and $\mathbf{t}_2$ scales as $\pm\Psi R_b$. Thus we find that

$$\langle \mathcal{W}r^2\rangle \sim \frac{L_b\Psi^2}{\mathcal{K}}\ . \qquad (39)$$

This implies that a polymer, such as DNA with a sharp hairpin is expected to display enhanced torsional fluctuations at its ends due to this amplification of the writhe fluctuations by the spontaneous curvature.

Similar modifications occur in the writhe dynamics: As before there are $N_1 = L_b/\ell_1$ dynamically independent sections on a polymer, each section moves a distance $\sqrt{\ell_1/\mathcal{K}}$. It is stretched a distance $\Psi\ell_1/L_b$ by the drift. Thus writhe fluctuations scale as

$$\langle(\mathcal{W}r(t) - \mathcal{W}r(0))^2 \sim N_1((\ell_1\Psi/L_b)\sqrt{\ell_1/\mathcal{K}})^2 \qquad (40)$$
$$\sim t^{1/2}\Psi^2/L_b\ , \qquad (41)$$

showing that this effect is most important in short, sharp bends.

9 Writhing of closed loops

Recently simulations have been performed [4] to study the writhing dynamics of short closed DNA

loops. Closure of the path in real space corresponds to adding a global constraint on the tangent

$$\oint \mathbf{t}(\sigma)\ \frac{d\sigma}{\kappa} = 0 \tag{42}$$

for all times. Here we consider the effect of this constraint on the statics and dynamics of writhe fluctuations for a short polymer such that $L \ll \mathcal{K}$.

The zero temperature configuration of the polymer on $\mathcal{S}_2$ is a great circle which we take to be the equator. From eq. (42) the average vertical position on the sphere can not change: Any motion of the polymer in the north-south direction must be compensated by a corresponding south-north motion elsewhere in the polymer so that the average vertical position of the polymer does not move. However on the sphere this is a *mass weighted* average with the "mass density" $1/\kappa$ (Note: The enclosed area is calculated with a unit weighted measure). By coupling fluctuations in density along the equator with transverse fluctuations in the position of the equator we can find a non zero contribution to the writhing.

The lowest order fluctuation in longitudinal density which does not violate the constraint of eq. (42) is proportional to $\cos 2\phi$ where ϕ is the azimuthal angle. From eq. (38) its amplitude scales as $\sqrt{L/\mathcal{K}}$. Coupling this density fluctuation to the transverse motions, also of magnitude $R_\sigma = \sqrt{L/\mathcal{K}}$ leads to a typical writhe fluctuation of $\pm L/\mathcal{K}$ for a closed loop. Thus we find that

$$\langle \mathcal{W}r^2 \rangle \sim L^2/\mathcal{K}^2. \tag{43}$$

in agreement with [24]

How does the closure constraint modify the writhing dynamics? The geometry is very similar to that discussed above for the bent open filament. There are $N_1 = N/\ell_1$ dynamic sections of length $2\pi\ell_1/L$ moving a distance $\sqrt{\ell_1/\mathcal{K}}$. Again the first order contribution must vanish, since the "mass weighted" position of the equator can not move. A non-zero term can be generated by coupling to the longitudinal density fluctuations of amplitude $\sqrt{L/\mathcal{K}}$:

$$\langle (\mathcal{W}r(t) - \mathcal{W}r(0))^2 \rangle \sim \ell_1^2/\mathcal{K}^2 \sim t^{1/2}\ . \tag{44}$$

The absolute magnitude to the fluctuations is thus decreased compared with the open polymer but the dynamic exponent for the fluctuations remains 1/2. Recently [4] molecular dynamics simulations were performed on a detailed microscopic model of DNA loops. The numerical results seem to be consistent with a square root of time evolution of the writhe-writhe correlation function.

10 Open Filaments

10.1 Relation with geometric phases

The geometry of figures (1,2) can be considered as a simple realisation of geometric phases which have been discussed in many field of physics. Examples in classical physics include Foucault's penduulum [25] and the nutation of tops. The best known example of these phases is however the Berry phase in optics and wave mechanics.

The geometry of fig. (1) is identical to that used to discuss the propagation of polarized light along bent fibre optics [26, 27, 28]: Consider a circular cross section optical fiber bent into the shape shown in fig. (1). If plane polarized light is sent down the fiber with the plane of polarization defined by the vector $\mathbf{n}$ then the polarization will be transported in exactly the same manner as the normal vector to the bar [9]. After the triple bend of fig. (1) the plane of rotation of the light has been rotated by $90°$. The rotation of the plane of rotation in fibre optics has been extensively studied as a simple example of the Berry or geometric phase. Berry's results on the existence of non-trivial phase factors is mathematically related to Fuller's theorem for writhe. While the geometry of the two situations seems very similar the geometric phase corresponding to this experimental situation is somewhat disguised so we shall now show how the rotation of the plane of polarization of light is equivalent to a phase shift for a photon.

There are two equivalent mathematical descriptions available for polarized light: Firstly, planar polarized waves, secondly circularly polarized photons. Using as a basis the planar representation with eigenstates $\phi_h = (1,0)$ and $\phi_v = (0,1)$, the helical eigenstates are $\phi_r = \frac{1}{\sqrt{2}}(1,i)$ and $\phi_l = \frac{1}{\sqrt{2}}(1,-i)$. Both the pair $\{\phi_v, \phi_h\}$ and the pair $\{\phi_l, \phi_r\}$ form a complete orthonormal basis for describing arbitrary pure states of the light. Consider an experimental set up that rotates the vector ϕ_h by an angle ψ. The new state is given by $(\cos\psi, \sin\psi)$. This state can also be expressed as a linear combination of the circularly

polarized states.

$$2\begin{pmatrix}\cos\psi\\ \sin\psi\end{pmatrix} = \exp(-i\psi)\begin{pmatrix}1\\ i\end{pmatrix} + \exp(i\psi)\begin{pmatrix}1\\ -i\end{pmatrix}. \tag{45}$$

The rotation of the plane of polarization is due to the modification of the relative phases of the two helical states. One state is advanced by ψ the second is retarded ψ. When a beam of circularly polarized light is sent down a fiber there is a phase shift which is equal to the writhe of the fibre times the helicity of the photon. This is a Berry phase.

A treatment of the geometry of writhe via a phase leads to an immediate generalization of Fuller's theorem for trajectories which are not closed on the sphere [29, 27]: The rotation angle between $\mathbf{n}(0)$ and $\mathbf{n}(L)$ is for the moment undefined if $\mathbf{t}(0)$ and $\mathbf{t}(L)$ are not parallel. This is because we have only defined parallel *locally* on $\mathcal{S}_2$ via parallel transport. We shall now see how find a *global* definition of parallel by noting that the phase phase difference between two helical states is unambiguous even if the trajectory does not close on $\mathcal{S}_2$: The phase shift in a fiber with arbitrary boundary conditions corresponds to the following recipe for calculating the writhe of the filament [29]: Follow the path $\mathbf{t}(0)$ to $\mathbf{t}(L)$ then close the path from $\mathbf{t}(L)$ to $\mathbf{t}(0)$ by a great circle (or geodesic). The phase shift is given by the area enclosed by the path $\mathbf{t}(0) \to \mathbf{t}(L)$ augmented by the great circle $\mathbf{t}(L) \to \mathbf{t}(0)$.

This recipe, fig. (5) has a interpretation on the sphere $\mathcal{S}_2$, for the writhing of a stiff polymer. Consider a path $\mathbf{t}(0)$ to $\mathbf{t}(L)$. The choice of $\mathbf{n}(0)$ is arbitrary for the calculation of the rotation, for convenience let us choose $\mathbf{n}(0)$ to that it points towards $\mathbf{t}(L)$. The three vectors $\mathbf{t}(0)$, $\mathbf{t}(L)$ and $\mathbf{n}(0)$ define a plane. Choose a reference vector, $\mathbf{v}(L)$, on the sphere at $\mathbf{t}(L)$ so that it is the "most parallel" possible to $\mathbf{n}(0)$. We choose $\mathbf{v}(L)$ so that it is coplanar with $\mathbf{t}(0)$ $\mathbf{t}(L)$ and $\mathbf{n}(0)$. This *definition* of *parallel* for two points on the sphere separated by a finite distance allows a definition of writhe for arbitrary free boundary conditions, leading to the geodesic recipe for calculating the writhe.

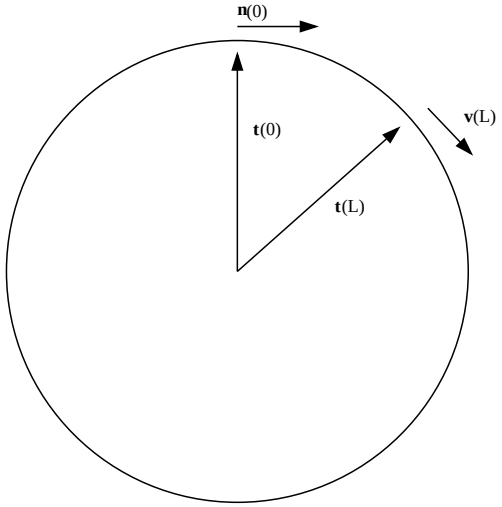

Figure 5: Geometry of an open trajectory on $\mathcal{S}_2$. The vectors $\mathbf{t}(0)$, $\mathbf{t}(L)$ and $\mathbf{n}(0)$ can be chosen to be co-planar. The vector $\mathbf{v}(L)$ is a reference vector at the point $s = L$ which allows one to compare rotations with $s = 0$. The "most parallel" choice possible for $\mathbf{v}(L)$ is shown in the figure, and is coplanar with the other vectors in this figure.

10.2 Perturbative treatment of open filaments

For short filaments there is an alternative derivation of the result that the path on the sphere must be closed by a geodesic. We shall use standard techniques from time dependent quantum mechanics, valid in the limit $L/\mathcal{K} \ll 1$. We proceed by studying eq. (2) for the case of a general matrix, $\Omega(s)$, describing both bend and twist, with $\Omega_{i,j} = \epsilon_{ijk}\omega^k$. If the average direction of the polymer is aligned in the $\hat{\mathbf{e}}_z$ direction the angular velocities ω^x and ω^y correspond to bending the filament, ω^z is the twist. We iteratively integrate this equation. The lowest order writhing contribution to rotations about the z-axis comes in second order.

$$\Omega(\mathcal{W}r) = \frac{1}{2}\int_0^L ds ds' \; \theta(s-s') \; (\omega_s^x \omega_{s'}^y - \omega_{s'}^x \omega_s^y). \tag{46}$$

This is just the time ordered commutator of the rotation operators familiar from quantum perturbation theory. Integrating by parts to transform the θ-function into a δ-function gives

$$\Omega(\mathcal{W}r) = \frac{1}{2}\hat{\mathbf{e}}_z . \left(\int_0^L (\dot{\mathbf{t}} \wedge \mathbf{t}) ds + \mathbf{t}(0) \wedge \mathbf{t}(L)\right) \tag{47}$$

For a closed curve on $\mathcal{S}_2$ the first term is the area enclosed by the curve $\mathbf{t}(s)$ on a patch of a sphere in agreement with Fuller's theorem: It is the first term

in the expansion of eq. (31). The second boundary term, due to the integration, present when the curve is open corresponds to closing the path by a geodesic from $\mathbf{t}(L)$ to $\mathbf{t}(0)$.

10.3 Dynamics of open filaments

This definition of writhe has interesting consequences on the measurement of writhe fluctuations on freely fluctuating filaments. When the ends of the filament were constrained we showed that the writhing was due to a series of N_1 small fluctuations distributed along the chains. If $\mathbf{t}(L)$ can also fluctuate there is a new contribution due to the modification in the closing of the path. In a time t the tangent $\mathbf{t}(L)$ moves $\sqrt{\ell_1/\mathcal{K}}$ sweeping out an area $\sqrt{\ell_1/\mathcal{K}} \times \sqrt{L/\mathcal{K}}$ thus there is an extra contribution to the writhing dynamics which scales $\langle \mathcal{W}r^2 \rangle \sim \ell_1 L/\mathcal{K}^2$ as before but coming from a single large end event rather than the sum of independent contributions.

11 Conclusion

We have shown that the writhing properties of a stiff polymer can be calculated from the well known properties of Gaussian random walks on a sphere. The predictions that $\langle \mathcal{W}r^2 \rangle \sim L^2$ and $\langle (\mathcal{W}r(t) - \mathcal{W}r(0))^2 \rangle \sim t^{1/4} L$ for short filaments should be accessible to micromanipulation techniques on actin filaments, or perhaps DNA, either by studying the rotational dynamics of the end of a marked polymer or by direct observation of the shape fluctuations occurring in three dimensions via confocal microscopy. As pointed out in recent work [3] disorder can sometimes have strong effects on the dynamics of twist and torsional modes. It would be interesting to have a better understanding of the effect of disorder on the correlation functions discussed here.

All real biopolymers have a helical structure with anisotropic bending elasticity. It is quite easy to treat this problem in the present description of diffusion on a sphere by introducing anisotropic diffusion coefficients on the sphere.

I wish to thank P. Olmsted for discussions on the relationship between geometric phases and Fuller's theorem, N. Rivier for discussions on Fermi-Walker (or parallel) transport, D. Beard for sending me his raw simulation on writhe fluctuations of DNA loops, A. Lesne for references on the distribution of winding angles.

References

[1] A.C. Maggs cond-mat/9712053 (1997).

[2] R. E. Goldstein, T. R. Powers, C, H. Wiggins, *Phy. Rev. Let*, **80**, 5232, (1998).

[3] J. D. Moroz, P. Nelson, *Macromol.* **31**, 6333, (1998).

[4] D.A. Beard, T. Schlick, *J. Chem. Phys*, **112**, 7323, (2000). I thank the authors for sending me their raw data to establish this point.

[5] F.B. Fuller, *Proc. Natl. Acad. Sci.* **68**, 815, (1971), *Proc. Natl. Acad. Sci* **75**, 3557, (1975).

[6] J.H. White *Am. J. Math.* **91** 693 (1969).

[7] Herbert Goldstein, *Classical Mechanics*, (Addison-Wesley, 1980).

[8] H.S.M. Coexter, *Introduction to Geometry*, (John Wiley & Sons, 1989).

[9] J. Segert, *Phys. Rev. A.* **36**, 10, (1987).

[10] W.M. Boothby, *An introduction to differentiable manifolds and Riemannian geometry*, (Academic Press, 1986).

[11] J.H. Hannay, *J. Phys. A*, **31**, L321, (1998).

[12] M. Doi and S.F. Edwards, *The theory of polymer dynamics*, (Oxford science publications, 1995).

[13] R.L Bishop, *American. Math. Monthly.* **82**, 246, (1975).

[14] P. Levy, *Processus Stochastiques et Mouvement Brownien*, (Paris: Editions Jacques Gabay, 1948).

[15] M.D. Frank-Kamenetskii, A.V. Vologdskii, *Sov. Phys. Usp.* **24**, (1981).

[16] F. Julicher, *Phys Rev.* **E 49**, 2429, (1994).

[17] J. Marko *Phys. Rev. E* **55**, 1758 (1997).

[18] C. Bouchiat and M. Mézard, *Phys. Rev. Lett.* **80**, 1556, (1998).

[19] F. Spitzer, *Trans. Am. Math. Soc* **87**, 187, (1958).

[20] M. Antoine, A. Comtet, J. Desbois, S. Ouvry, *J. Phys A.* **24** 2581, (1991).

[21] M.D. Barkley, B.H. Zimm, *J. Chem. Phys.*, **70**, 2991, (1979).

[22] A.C. Maggs, cond-mat/9912119 (1999).

[23] J.H. White, R.A. Lund, W.R. Bauer, Biopolymers. **38**, 235, (1996).

[24] I. Tobias. *Biophysical J.* **74** 2545 (1998).

[25] *Geometric phases in physics*. ed. A. Shapere, F. Wilczek. (World Scientific 1989).

[26] M.V. Berry, *Nature*, **326**, 277, (1987).

[27] F.D.M. Haldane, *Opt. Lett.* **11**, 730, (1986).

[28] A. Tomita, R. Y. Chiao, *Phys. Rev. Lett*, **57**, 937, (1986).

[29] M.V. Berry, *J. Modern Optics* **34**, 1401 (1987).